

Fidelity of photon interferometry for recording the evolution of a nascent quark-gluon plasma

Dinesh Kumar Srivastava*

Theoretical Physics Institute, University of Minnesota, Minneapolis, Minnesota 55455

(Received 10 June 1993)

The fidelity of two-photon intensity interferometry for reflecting the dynamics of nascent quark-gluon plasma formed in a high energy nucleus-nucleus collision is examined. A $(3+1)$ -dimensional expansion of the plasma as well as a $(1+1)$ -dimensional expansion according to Bjorken hydrodynamics, both with a first order phase transition, are considered. The correlation of high transverse-momentum photons is shown to be a precision tool for the investigation of the space-time evolution of the high density QCD plasma. In particular, the longitudinal correlation function, which depicts the time development of the system, is seen to have its origin in two sources: one corresponding to the early plasma phase and the second to the later stages. This aspect may help identify thermal photons according to their "time of birth" during evolution.

PACS number(s): 12.38.Mh, 24.85.+p, 25.75.+r

I. INTRODUCTION

The primary motivation for colliding large nuclei such as gold or lead at high energies is to study the behavior of strongly interacting matter at high (energy) density. Such matter will expand rapidly and eventually break up into observable hadrons. The following scenario for the formation stage is by now considered to be rather standard: the two nuclei masquerading as clouds of valence and sea partons pass through each other, multiple parton collisions and parton production occur, leading to a (generally nonequilibrium) high density plasma of quarks and gluons [1]. This plasma expands, cools, and becomes more dilute, paving the way for hadronization [2]. Calculations based on lattice quantum chromodynamics (QCD) provide information about the transition of such matter from a state of deconfined colored quarks and gluons to one of color singlet hadrons. Such calculations, however, do not tell us anything about the actual evolution of the system produced in the nuclear collisions.

The most simple scenario, which is also the most exhaustively studied, is one in which the system, after some (early) thermalization time, remains in thermal equilibrium until the hadrons produced during the last stage of the evolution stop interacting. In this case the observed hadrons will reflect the properties of the *last* thermal stage of the equilibrium hadronic gas before the freeze-out, *irrespective of the nature of the early stages of the produced matter*.

High energy photons or large mass dileptons, on the other hand, are copiously produced during the early hot and dense stage. Since they are not affected by rescat-

tering they would provide *pristine* information about the *nascent* quark-gluon plasma (QGP). With this aspect in mind, a considerable effort has been devoted in investigating high energy photons as a possible signature of QGP.

For the same reasons it is felt that interferometry of high energy photons [3-5] would provide us the most direct view of the history of the space-time evolution of the QGP [6,7]. At present this seems to be the only possible means of getting accurate information about these aspects of the nascent QGP which unfortunately has only an ephemeral existence.

In the present work we investigate the feasibility of these studies in detail by looking at the correlations, first at the CERN Large Hadron Collider (LHC) energies and then as a function of the particle multiplicity density. We also emphasize that the longitudinal correlation function which depicts the time development of the source is seen to consist of two source terms: one having a shorter time scale corresponding to emissions from the QGP phase and the other having a longer time scale corresponding to emissions from the later, mixed, and hadronic phases. This aspect, which could indeed have interesting consequences in terms of the signatures of the phase transition, had escaped our attention in our earlier work [6,7].

II. DEFINITIONS AND FORMULATION

The correlation between two photons with momenta \mathbf{k}_1 and \mathbf{k}_2 and the same helicity is given by

$$C(\mathbf{k}_1, \mathbf{k}_2) = \frac{P(\mathbf{k}_1, \mathbf{k}_2)}{P(\mathbf{k}_1)P(\mathbf{k}_2)}, \quad (1)$$

where

$$P(\mathbf{k}) = \int d^4x \frac{dN(x, \mathbf{k})}{d^4x d^3k} \quad (2)$$

*Present and permanent address: Variable Energy Cyclotron Centre, 1/AF, Bidhan Nagar, Calcutta 700 064, India.

and

$$P(\mathbf{k}_1, \mathbf{k}_2) = \int d^4x_1 d^4x_2 \frac{dN(x_1, \mathbf{k}_1)}{d^4x_1 d^3k_1} \frac{dN(x_2, \mathbf{k}_2)}{d^4x_2 d^3k_2} \times [1 + \cos(\Delta \mathbf{k} \cdot \Delta \mathbf{x})] . \quad (3)$$

$dN(x, \mathbf{k})/d^4x d^3k$ is the rate per unit volume for producing a photon with momentum \mathbf{k} at the space-time point x . This expression assumes independent production of photons. We shall not consider photon energies so small that coherence effects need be included [3].

The correlation function $C(\mathbf{k}_1, \mathbf{k}_2)$ is often represented in terms of the longitudinal, outward, and sideward momenta differences of the two photons. Thus we have for the four-momentum k_i^μ of the i th photon:

$$k_i^\mu = (k_{iT} \cosh y_i, \mathbf{k}_i) \quad (4)$$

with

$$\mathbf{k}_i = (k_{iT} \cos \psi_i, k_{iT} \sin \psi_i, k_{iT} \sinh y_i), \quad (5)$$

where k_T is the transverse momentum, y is the rapidity, and ψ is the azimuthal angle. Now the difference of the transverse momenta \mathbf{q}_T is obtained as

$$\mathbf{q}_T = \mathbf{k}_{1T} - \mathbf{k}_{2T}, \quad (6)$$

and the average transverse momentum is

$$\mathbf{K}_T = (\mathbf{k}_{1T} + \mathbf{k}_{2T})/2. \quad (7)$$

Choosing the x axis to be parallel to \mathbf{q}_T we get

$$\begin{aligned} q_L &= k_{1z} - k_{2z} \\ &= k_{1T} \sinh y_1 - k_{2T} \sinh y_2, \\ q_{\text{out}} &= \frac{\mathbf{q}_T \cdot \mathbf{K}_T}{K_T} \end{aligned} \quad (8)$$

and

$$\begin{aligned} P_{ci} &= K \int d\tau \tau r dr d\eta d\phi T^2 \ln \left(\frac{2.9}{g^2} \frac{\gamma_T k_{iT} [\cosh(y_i - \eta) - v_T \cos(\phi - \psi_i)]}{T} + 1 \right) \\ &\times \exp(-\gamma_T k_{iT} [\cosh(y_i - \eta) - v_T \cos(\phi - \psi_i)]/T) \cos[(\Delta E \cosh \eta - q_L \sinh \eta)\tau - \mathbf{q}_T r \cos \phi]. \end{aligned} \quad (15)$$

P_{si} is given by a similar expression with the cosine replaced by a sine. These integrals have to be evaluated numerically.

We note that $q_T \neq 0$ controls the space-correlation and that $\Delta E \neq 0$ and/or $q_L \neq 0$ control the time correlation of the emitted photons.

If the transverse expansion of the flow can be neglected ($v_T = 0$) and additionally a Gaussian approximation is used for the integral involving the space-time rapidities,

$$= \frac{(k_{1T}^2 - k_{2T}^2)}{\sqrt{k_{1T}^2 + k_{2T}^2 + 2k_{1T} k_{2T} \cos(\psi_1 - \psi_2)}} , \quad (9)$$

$$\begin{aligned} q_{\text{side}} &= \left| \mathbf{q}_T - q_{\text{out}} \frac{\mathbf{K}_T}{K_T} \right| \\ &= \frac{2k_{1T} k_{2T} \sqrt{1 - \cos^2(\psi_1 - \psi_2)}}{\sqrt{k_{1T}^2 + k_{2T}^2 + 2k_{1T} k_{2T} \cos(\psi_1 - \psi_2)}} . \end{aligned} \quad (10)$$

For the emission rate of thermal photons we use the results of Ref. [8] (see also Ref. [9]) where it has been established that the rates in the hadronic phase and in the plasma phase are the same, within our present ability to calculate them, when compared at the same temperature T . We use the computed rate in the plasma phase, which is

$$E \frac{dN}{d^4x d^3k} = K T^2 \ln \left(\frac{2.9 E}{g^2 T} + 1 \right) \exp(-E/T), \quad (11)$$

where E is the photon energy, g is the QCD coupling constant, and K is a constant which is irrelevant for the correlation function.

The coordinate time and position are $x^\mu = (\tau \cosh \eta, r \cos \phi, r \sin \phi, \tau \sinh \eta)$ where τ is the proper time and r and ϕ are the radial coordinate and angle. The local flow velocity of the matter is given by

$$u^\mu = \gamma_T (\cosh \eta, v_T \cos \phi, v_T \sin \phi, \sinh \eta) , \quad (12)$$

where $\gamma_T = 1/\sqrt{1 - v_T^2}$ and v_T is the transverse velocity of the matter. This v_T and the temperature of the fluid element are obtained from numerical calculations of the flow [10–12] as functions of τ and r . Writing

$$P(\mathbf{k}_1, \mathbf{k}_2) = P_1 P_2 + P_{c1} P_{c2} + P_{s1} P_{s2} \quad (13)$$

we get, for the functions P_i and P_{ci} ,

these expressions can be further simplified [6] to yield

$$\begin{aligned} P_i &= P(\mathbf{k}_i) = \pi R^2 K \int d\tau \tau \sqrt{\frac{2\pi T}{k_{iT}}} T^2 \ln \left(\frac{2.9 k_{iT}}{g^2 T} + 1 \right) \\ &\times \exp(-k_{iT}/T) \end{aligned} \quad (16)$$

and

$$\begin{aligned}
P_{ci} &= \pi R^2 K \int d\tau \tau \sqrt{\frac{2\pi T}{k_{iT}}} T^2 \ln \left(\frac{2.9 k_{iT}}{g^2 T} + 1 \right) \\
&\times \exp(-k_{iT}/T) \left[\frac{2J_1(q_T R)}{q_T R} \right] \\
&\times \cos[(\Delta E \cosh y_i - q_L \sinh y_i)\tau]. \quad (17)
\end{aligned}$$

Here J_1 is the Bessel function, R is the radius of the identical nuclei undergoing a central collision, and

$$\Delta E = k_{1T} \cosh y_1 - k_{2T} \cosh y_2, \quad (18)$$

$$q_T = |k_{1T} \cos \psi_1 - k_{2T} \cos \psi_2|. \quad (19)$$

The P_{si} are the same as the P_{ci} with the substitution of a sine for the cosine. The space-correlation, which is decided by $q_T \neq 0$, is fixed for the *no transverse flow* condition [13] envisaged here if $\Delta E = q_L = 0$. For this we get a very simple expression

$$C(\mathbf{k}_1, \mathbf{k}_2, q_L = 0, q_{out} = 0) = 1 + \left[\frac{2J_1(q_{side} R)}{q_{side} R} \right]^2, \quad (20)$$

where now $q_{side} = k_T |\cos \psi_1 - \cos \psi_2|$. This configuration obviously allows one to infer the radius of the emitting system. The typical scale of q_{side} is seen to be $1/R \approx 20$ MeV for collisions involving lead nuclei. We also note that the correlation function for this configuration depends on q_{side} alone, and thus its experimental determination can be facilitated by an integration of the rates over a large phase space. We may also recall [6] that for the case of *no transverse flow*, photons having $k_T \gg T_i$ are predominantly produced in the plasma and

the correlation function for small values of q_L can be approximated as

$$\begin{aligned}
C(\mathbf{k}_1, \mathbf{k}_2, q_{out} = q_{side} = 0) \\
\approx 1 + \cos [4k_T \tau_i \sinh^2(\Delta y/2)]. \quad (21)
\end{aligned}$$

This illustrates that the longitudinal correlator for photons can be used to infer the dimensions of the initial space-time extent of the system [6]. This is in stark contrast to the situation for hadron interferometry where the scales for the three correlators are similar [14] due to their sensitivity to the dimensions of the system at the instant of freeze-out.

We use the following criterion of isentropic expansion for the particle rapidity densities:

$$T_i^3 \tau_i = \frac{2\pi^4}{45\zeta(3)\pi R^2 4a_Q} \frac{dN}{dy_\pi} \quad (22)$$

along with $\tau_i = 1/3T_i$ as suggested by uncertainty principle. In the above dN/dy_π is the pion rapidity density, R is the transverse dimension of the system and $a_Q = 37\pi^2/90$ for a system of u and d quarks. We choose $T_c = 160$ MeV and $T_f = 140$ MeV. Thus, for example, we have $T_i = 958$ MeV, $\tau_i = 1/3T_i = 0.069$ fm/c corresponding to a particle rapidity density of 5624 in the central region [15,11] for a collision involving two lead nuclei. Other details of calculations can be obtained in our earlier work. This model and these numbers are used for illustrative purposes.

It is interesting to note that the time integrals in the functions $P(\mathbf{k}_1, \mathbf{k}_2)$ can be split as follows:

$$\begin{aligned}
P(\mathbf{k}_1, \mathbf{k}_2) &= \int_{\tau_i}^{\tau_Q} d\tau_1 \int_{\tau_i}^{\tau_Q} d\tau_2 [\dots] + \int_{\tau_Q}^{\tau_H} d\tau_1 \int_{\tau_Q}^{\tau_H} d\tau_2 [\dots] + \int_{\tau_H}^{\tau_F} d\tau_1 \int_{\tau_H}^{\tau_F} d\tau_2 [\dots] \\
&+ \left(\int_{\tau_i}^{\tau_Q} d\tau_1 \int_{\tau_Q}^{\tau_H} d\tau_2 [\dots] + \int_{\tau_i}^{\tau_Q} d\tau_1 \int_{\tau_H}^{\tau_F} d\tau_2 [\dots] + \int_{\tau_Q}^{\tau_H} d\tau_1 \int_{\tau_H}^{\tau_F} d\tau_2 [\dots] + 1 \leftrightarrow 2 \right). \quad (23)
\end{aligned}$$

In the above τ_Q denotes the end of the QGP phase, τ_H the end of the mixed phase, and τ_F the time of freeze-out. This explicitly provides for three source terms having their origin in the plasma, the mixed phase and the hadronic phase, respectively. The widely different time scales for the plasma phase as compared to the later phases has been noted earlier [6,7]. For very different time scales operating in the three sources it is likely that the interference terms may not be large at least for the longitudinal correlation. The relative strength of the three sources should then decide the correlation function. We shall see later that it is indeed so.

All the results presented in this work assume that the polarization of each photon is known. If a polarization average is taken instead, then the factor $1 + \cos(\Delta \mathbf{k} \cdot \Delta \mathbf{x})$ in Eq. (3) gets replaced by $1 + \frac{1}{2} \cos(\Delta \mathbf{k} \cdot \Delta \mathbf{x})$. This

means that $C \rightarrow \frac{3}{2}$ at zero relative momentum rather than 2. Otherwise the behavior of the correlation function would remain unchanged.

III. RESULTS FOR LHC ENERGIES

It is our intention to gauge the extent to which the interferometry of photons truthfully reflects the space-time development of the nascent quark-gluon plasma.

In order to check this, we summarize the temperature profile of the system at $z = 0$ at different times [Figs. 1(a) and 1(b)] as obtained from the hydrodynamic calculations including the transverse flow for the initial conditions envisaged at LHC energies in collisions involving

two lead nuclei. We note a very interesting development. We see that at very early times the part of the surface which encloses the highest temperatures moves inward with the passage of time, whereas the part which encloses lower temperatures moves outward. However at later times after the entire fluid has cooled to the transition temperature, this surface starts moving in. As a consequence, observables sensitive to highest temperatures and hence earliest times see a decreasing transverse radius.

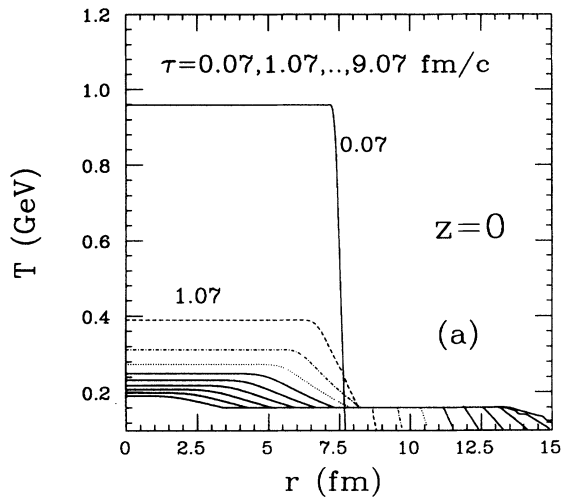
In Fig. 2(a) we show the correlation function for $k_{1T} = k_{2T} = 1, 2, 3,$ and 4 GeV and $y_1 = y_2 = 0$ as a function of q_{side} for the plasma alone. The results for the case of no transverse flow are also shown. These results corresponds

to the configuration $\Delta E = q_L = q_{\text{out}} = 0$ and $q_T = q_{\text{side}}$.

We see that during the quark-gluon plasma phase, the photons having smallest transverse momenta are emitted from sources having smallest transverse dimensions ($\sim 1/\bar{q}_{\text{side}}$). Recalling that the photons having smaller transverse momenta are emitted from cooler environs, we note that the inward movement of the high temperature profile during this phase is clearly reflected by the correlation function.

However, the correlation function provided by the experiments will be a result of integration over the entire history of the plasma as thermal photons are also emit-

Temperature Profile at LHC: Early Times



Temperature Profile at LHC: Late Times

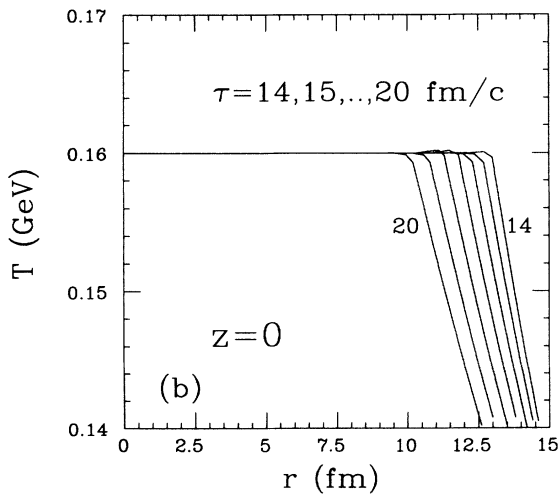
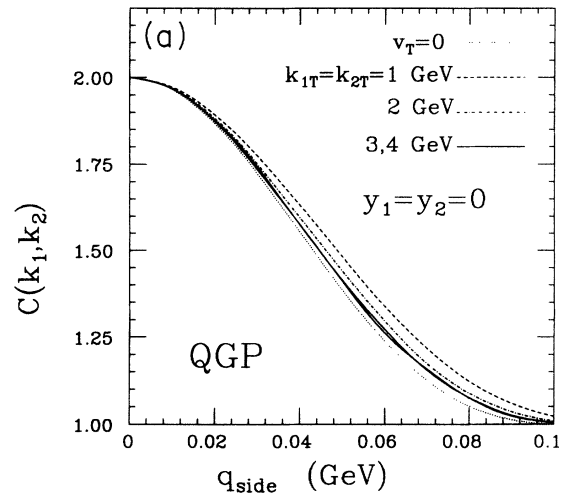


FIG. 1. (a) Temperature profile of the transversely expanding system of quark-gluon plasma at LHC energies at early times, when the temperature is still high. All the results are for collision of two lead nuclei. (b) Temperature profile of the transversely expanding system of quark-gluon plasma at LHC energies at late times, when the temperature is rather low.

Transverse Dimensions at LHC : Side



Transverse Dimensions at LHC : Side

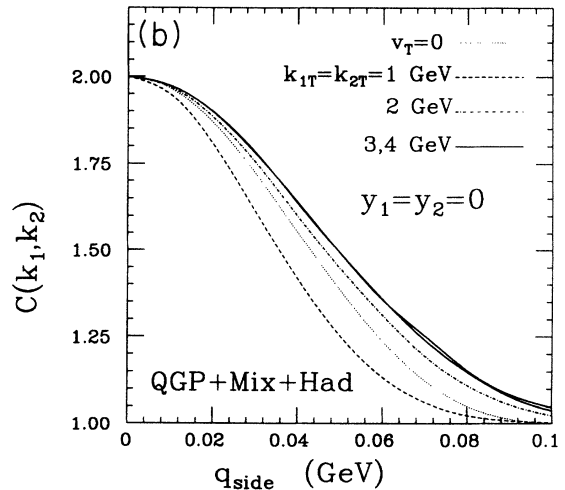


FIG. 2. (a) Sideward correlation function for the photons emitted (at LHC energies) during the quark-gluon plasma phase only, for $k_T = 1, 2, 3,$ and 4 GeV. Results for no transverse flow are also given. (b) Sideward correlation function for the photons emitted (at LHC energies) during the entire history of the interacting system plasma phase only, for $k_T = 1, 2, 3,$ and 4 GeV. Results for no transverse flow are also given.

ted from the mixed phase and the hadronic phase during which the evolution characteristics are quite different. The resulting correlation function is shown in Fig. 2(b). Now we find that while the photons having transverse momenta of 2, 3, or 4 GeV are providing a source size smaller than the original dimension of the nuclei, those having the transverse momentum of 1 GeV, being emitted till much later, give a source size larger than the original dimension. This obviously reflects the fact that at LHC energies photons having transverse momenta of 4, 3, or even 2 GeV have a large contribution from the plasma phase when the surface enclosing the hot (enough) environs is shrinking, whereas those having a transverse momentum, say, 1 GeV, derive their leading contribution from the mixed phase and the hadronic phase when

the relevant volume is expanding.

The fidelity of photon interferometry in reflecting the temporal development of the quark-gluon plasma is seen from Fig. 3(a), where we have shown the correlation as a function of the longitudinal momentum difference q_L . The results correspond to the configuration $q_{out} = q_{side} = 0$. The ‘‘longitudinal dimension’’ determined by $1/\bar{q}_L$ is seen to decrease with the increase of the transverse momentum. The typical scale associated with this length is seen to be of the order of a GeV. A similar result had earlier been noted at energies reached at the BNL Relativistic Heavy Ion Collider (RHIC) (see Figs. 7(a)–7(d), Ref. [7]).

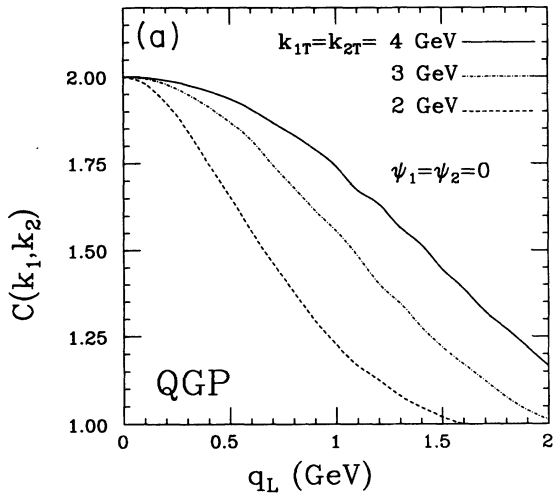
Finally the correlation for photons emitted during the entire history of the system is given in Fig. 3(b). Now we note that the longitudinal dimensions provided by the photons decreases with increase in their transverse momenta, and the typical scale is reduced to about 1/2 GeV. This can be most easily seen by plotting $\ln(C - 1)$ as a function of q_L^2 . The most interesting aspect of these correlation functions is that they are clearly seen to have their origin in mainly two sources having different time scales; that is,

$$C \sim 1 + a \exp(-\alpha^2 q_L^2) + b \exp(-\beta^2 q_L^2)$$

+interference terms (24)

with $\alpha > \beta$. As we know the history of evolution in these model studies, we immediately realize the source term with the scale $1/\alpha$ gives the emissions from the later stages of the system, whereas the term with the scale $1/\beta$ gives contributions from the early QGP phase of the plasma. We also note that the source strength b for the QGP, increases with the transverse momentum, indicating the dominant contribution of the plasma to

Longitudinal Dimensions at LHC



Longitudinal Dimensions at LHC

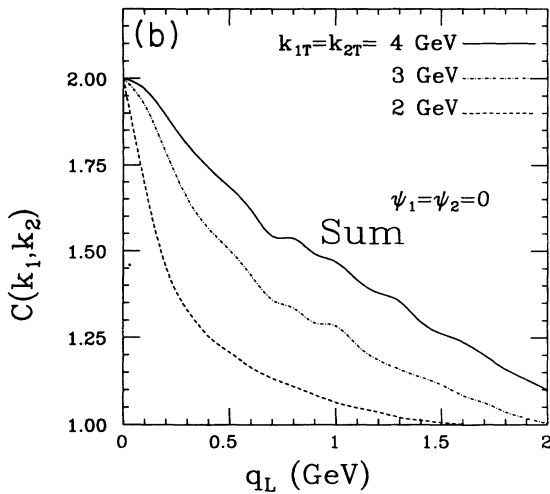


FIG. 3. (a) Longitudinal correlation function at LHC energy for a transversely expanding system for photons having different k_T for the QGP phase only. (b) Longitudinal correlation function for the entire history of the system for $k_T = 2, 3,$ and 4 GeV.

Trans. Dim. vs. Initial Time at LHC : Side

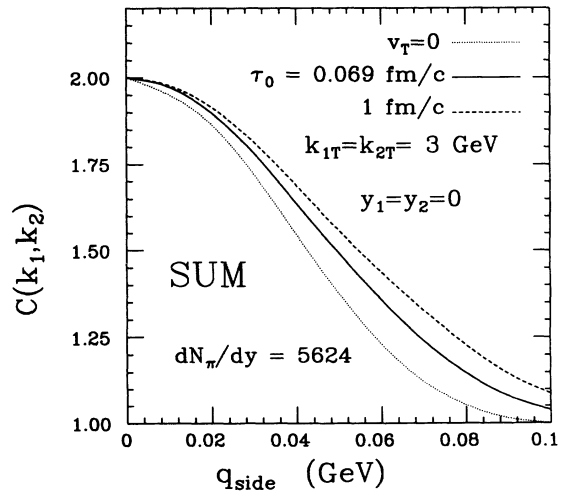


FIG. 4. Sideward correlation function for the entire history of the system at LHC energies for $k_T = 3$ GeV. Two different initial times; $1/3T_i$ and 1 fm/c have been used.

Long. Dim. vs. Initial Time at LHC

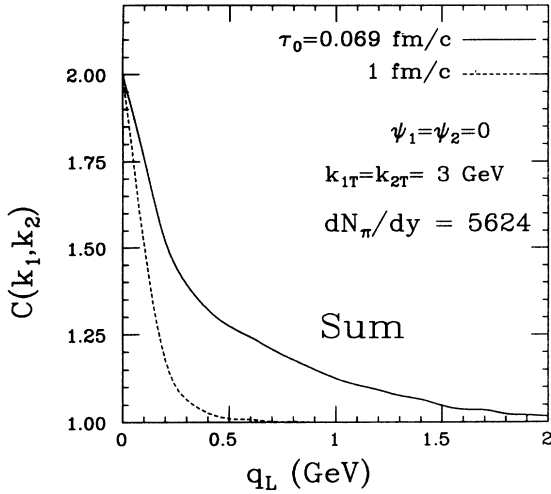


FIG. 5. Longitudinal correlation function for the entire history of the system at LHC energies for $k_T = 3$ GeV. Two different initial times $1/3T_i$ and 1 fm/c have been used.

photons having larger transverse momenta. These aspects, we feel, can be developed as a means to tag the thermal photons according to their origin in space and time.

There is a debate in the literature about the initial time τ_i (see the discussion in [6]). Prescriptions vary from $\tau_i = 1/3T_i$ to a few fm/c. In order to check the sensitivity of photon interferometry to these details we show in Fig. 4 the sideward correlation function for 3 GeV photons for two initial times: 0.069 fm/c and 1 fm/c, constrained by the requirement of multiplicity density given earlier [Eq. (22)]. We find that the 3 GeV photons which would be predominantly emitted by the hot plasma see an effectively smaller source size if the initial time is larger. This is easily understood by looking at the temperature profiles in Fig. 1(a), and realizing that for $\tau_i = 1$ fm/c, the plasma having higher temperatures would be limited to relatively smaller sizes.

Considering that photon interferometric studies may not be easy, we give the results for the longitudinal correlation function in Fig. 5 which are even more dramatic. The two scales for the longitudinal correlation function referred to earlier [Eq. (24)] are seen quite clearly. We also note that the smaller formation time, which implies a larger initial temperature and hence a larger contribution from the plasma changes the correlation function considerably. This implies a unique sensitivity of the photon interferometry to the initial times for the nascent plasma.

IV. EVOLUTION OF SOURCE WITH PARTICLE MULTIPLICITY DENSITY

We have already seen that for the multiplicity density considered appropriate for LHC energies for collisions involving two lead nuclei, photon interferometry can be

effectively utilized to probe the history of quark-gluon plasma.

In this section we study the evolution of the source as a function of the multiplicity and, most importantly, we count the number of thermal photon pairs available for this study.

In Fig. 6 we have plotted the number of thermal photons as a function of transverse momentum for different pion multiplicity densities. Only longitudinal expansion according to the Bjorken hydrodynamics is used. The initial time and temperature are constrained according to Eq. (22) as discussed earlier. We see the well-understood change of slope around 2 GeV [16], and increased production of photons from the quark-gluon plasma phase at larger k_T .

The corresponding results for the evolution with a $(3+1)$ -dimensional expansion are shown in Fig. 7. Two aspects of the results are immediately seen. First, the change of slope beyond the transverse momentum of about 2 GeV is much more gentle now, and most noticeably, the results for higher transverse momenta are not drastically different for the two cases. This later aspect has its origin in the dominance of photons having their origin in the quark-gluon plasma for higher transverse momenta. Recall though, that for cases involving transverse expansion, the photons having their origin in the hadronic matter make a substantial contribution [11] for moderate transverse momenta due to the transverse kick they receive from the flow. Photon interferometry can help us to isolate these photons by virtue of its selection of photons having smallest *relative* transverse momenta [7]. The relative momenta of the photons from the hadronic matter increases rapidly with the distance in their origin, as the system is in rapid transverse expansion during the later stages of the evolution.

In Fig. 8 we have plotted the sideward correlation as

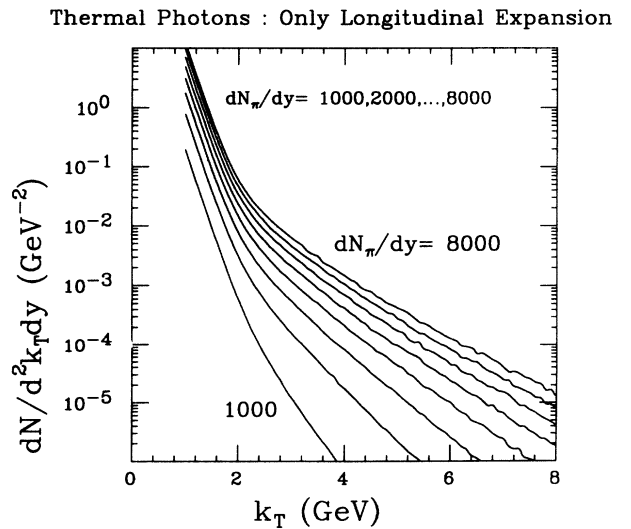


FIG. 6. Thermal photons for different multiplicities, with only a longitudinal expansion according to Bjorken hydrodynamics. The initial time $\tau_i = 1/3T_i$, and the multiplicities are constrained according to Eq. (22).

Thermal Photons : With Transverse Expansion

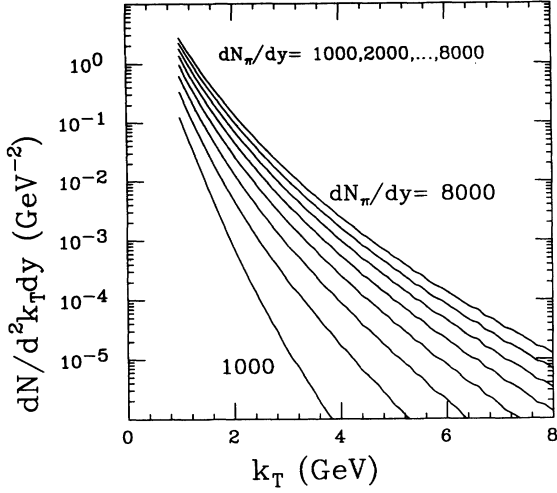


FIG. 7. Thermal photons for different multiplicities, with a (3 + 1) dimensional expansion. The initial time $\tau_i = 1/3T_i$, and the multiplicities are constrained according to Eq. (22).

seen by 2 GeV photons for multiplicity density ranging from 3000 to 5000. Results for the situation not involving transverse expansion are also given. A rich scenario is seen to emerge. The transverse dimension of the system as measured by $1/\bar{q}_{\text{side}}$ is seen to be largest for $dN/dy_\pi = 3000$ and smallest when the particle rapidity density is 5000. We can understand this as follows. The initial temperature increases with the pion multiplicity. However, very high temperatures are not needed for producing 2 GeV photons. When $dN/dy_\pi = 3000$ the photons even from the late (cool) stages in the development of the system appear in the k_T window at 2 GeV by taking

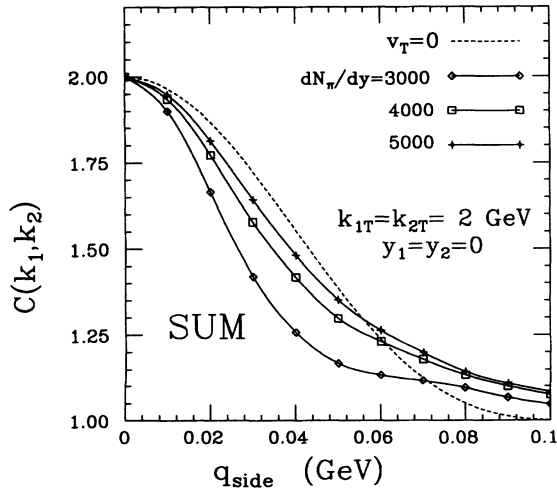
Transverse Dimension vs. dN_π/dy : Side

FIG. 8. Sideward correlation function for the entire history of the system as a function of the pion multiplicity density for $k_T = 3$ GeV.

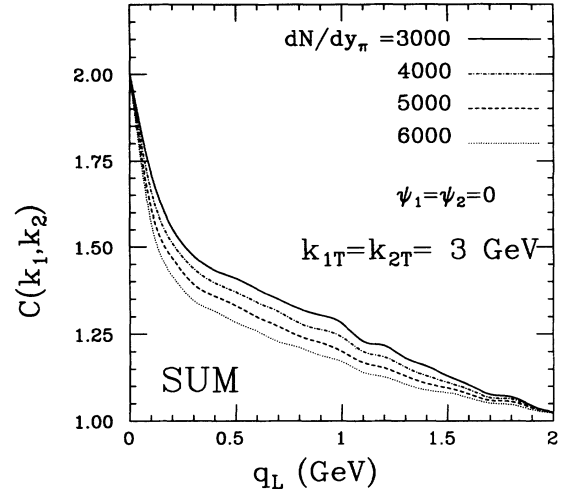
Longitudinal Dimensions vs. dN/dy_π 

FIG. 9. Longitudinal correlation function for the entire history of the system as a function of the pion multiplicity density for $k_T = 3$ GeV.

advantage of the transverse velocity of the system, when the effective dimension of the system is large. For higher multiplicities the system remains in thermal contact till longer times, and then the transverse dimensions of the system have already started decreasing, though they are still larger than the original dimensions. Such sensitivity to the details of the evolution is unique for photons. With the availability of such a precision tool it would indeed be interesting to have the photons map the entire mosaic of the evolution.

In Fig. 9 we have given results for the longitudinal correlation studied by photons having a transverse momentum of 3 GeV, when particle rapidity density is increased from 3000 to 6000. We see the characteristic two-source correlation function depicting the time development of the system. We note that the time scale associated with the plasma part of the source function [see Eq. (24) above] decreases with the increase in multiplicity, as indeed it is built into the model used here.

V. DISCUSSION AND CONCLUSION

In order to study the feasibility of photon interferometry experiments we show in Fig. 10, the number of photon pairs having transverse momenta ≥ 1 GeV and $|y| \leq 1$ as a function of pion multiplicity density for a transversely expanding plasma. The initial time and temperature are constrained by Eq. (22) as before. Results are also given for the case of a (1 + 1)-dimensional expansion. The number of thermal photon pairs is seen to increase rapidly as $(dN/dy_\pi)^4$, and it is felt that enough statistics may be generated for a meaningful analysis of the results for interferometry at LHC where a few hundred central events may be generated every second. Considering the accuracy with which the photon interferometry reflects the space-time evolution of the system and the fact that

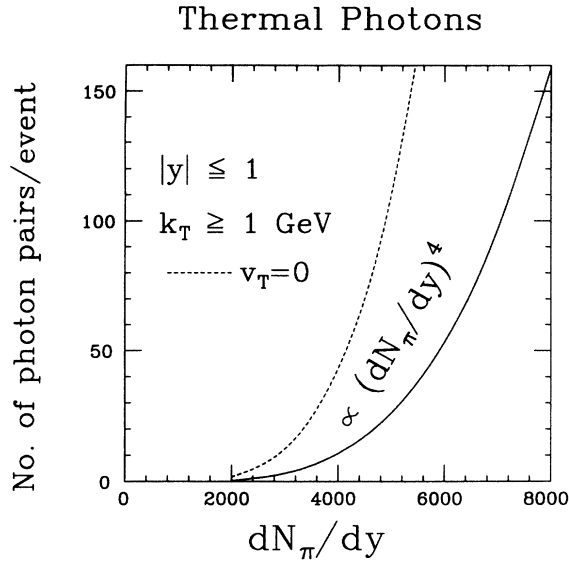


FIG. 10. Number of thermal photon pairs having transverse momenta greater than or equal to 1 GeV and rapidity $|y| \leq 1$. We see that it increases rapidly as $(dN/dy_\pi)^4$. Results for a purely longitudinal expansion are also given.

this seems to be the *only* way to get this information about the *nascent* quark-gluon plasma, it will only be prudent to plan for such an experiment well in advance.

The question of background (which, if too large, would destroy the beautiful tool of photon interferometry) has already been discussed in Refs. [6,7] in detail, and we do not wish to repeat them here.

We would like to recall though that γ/π^0 , which provides a measure of the difficulty of detecting direct photons, for *AA* collisions may not be same as for *pp* collision. Effects such as decay, degradation, or absorption of (mini)jets in the hot and dense hadronic matter in the *AA* collisions may largely suppress the high transverse momentum tail in the π^0 spectrum and enhance the thermal photon signal.

We may also recall an interesting speculation that the pion densities achieved in very energetic heavy ion collisions may exceed the critical density for Bose-Einstein condensation. This can have dramatic effect for π^0 spectra, where the absence of the Coulomb repulsion may cause a collapse of all of them into an extremely low momentum state $\Delta p \sim 1/R$, where R is the size of the system at freeze-out. This will reduce the background of decay photons at larger transverse momenta enormously and make the task of detecting thermal photons and so also photon interferometry somewhat easy. At the same time it is also felt that final-state interactions affecting the hadronic interferometry may also be considerably enhanced with the increase of the particle multiplicity.

In principle, one could perhaps calculate the spectrum for π^0 from the hydrodynamical calculations which provided the basis for the flow effects for photons in the above. This, however, will have a number of uncertainties. First, such a treatment will not incorporate the

pions produced in (mini)jets, which should become increasingly important at higher incident energies. Second, it is not clear as to what value of freeze-out temperature would be most appropriate for such strongly interacting particles as pions. It should be kept in mind that a greatly enhanced transverse dimension of the system due to the transverse expansion may lead to a much reduced freeze-out temperature if the usual requirement of mean free path being larger than the transverse dimensions of the system is applied. The equation of state for the hadronic matter used for the hydrodynamic treatment will become invalid at temperatures much lower than the pion mass. It will also not be possible for us to use [Eq. (11)] at much lower hadronic temperatures. In any case it should be kept in mind that as the rate of production of thermal photons is a strongly increasing function of the temperature, their production would become feeble well before the pions freeze-out. These questions can possibly be settled only if detailed experimental data on pionic distribution are available.

It is also felt that the problem associated with the background from decay photons (from say, π^0) may not be very severe at larger transverse momenta considered here. These naive expectations can be put on a more quantitative footing by evaluating the correlation functions for decay photons obtained from one of the event generators such as VENUS or FRITOF. Such an exercise is in progress.

For the present we shall assume that the distribution of pions at the time of freeze-out can be obtained by assigning an appropriate inverse slope to their “ m_T ” distribution. This inverse slope should account for the transverse velocity of the hadronic fluid at the time of freeze-out [11]. In Figs. 11 and 12 we show the thermal photon vs

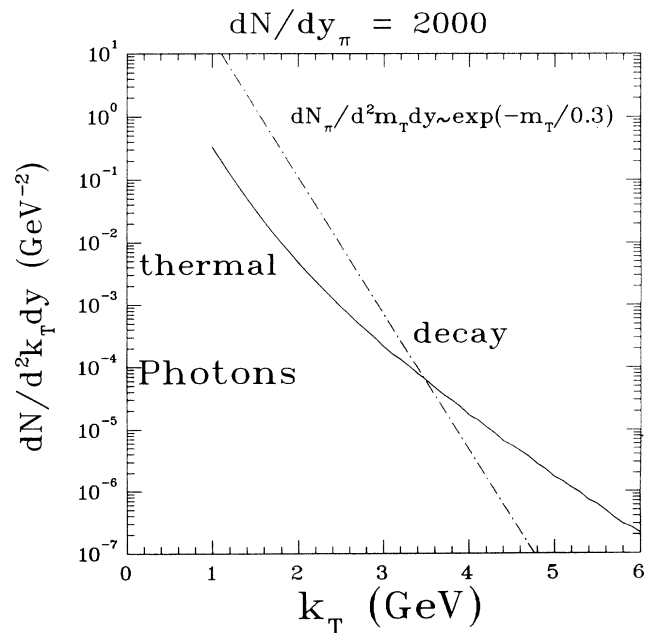


FIG. 11. Thermal photons vs decay photons for $dN_\pi/dy = 2000$. One third of the pions are taken as π^0 and their transverse mass distribution is assigned an inverse slope of 300 MeV.

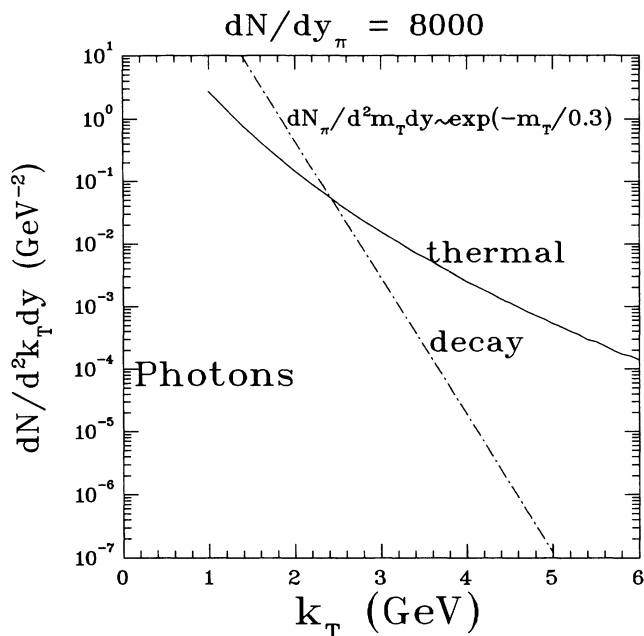


FIG. 12. Same as Fig. 11, for $dN_\pi/dy = 8000$.

decay photon spectrum for such an exercise by assigning an inverse slope of 300 MeV [1] to the pion spectrum when $dN_\pi/dy = 2000$ and $dN_\pi/dy = 8000$. The earlier multiplicity is appropriate for RHIC energies and the later for LHC energies.

We see that the optimum conditions for performing high energy photon interferometry studies are obtained at LHC energies. Recalling the fact that the inverse slope of 300 MeV is rather large for RHIC energies, the situ-

ation is not exactly hopeless there either for performing such studies. It will not be easy though. However if we argue that a large part of the decay photons could be identified as such by the invariant mass analysis, then we should perhaps compare the thermal photon spectrum with only a small percentage of the decay photon spectrum to get an idea of the background which remains to be tackled [7].

The unique sensitivity of the photon interferometry seen in the present work could also be used to check the validity of hydrodynamic expansion employed here. One may use it to check the other alternative, a cascade model of the mixed and final hadronic phases, which makes no assumptions about the maintenance of local equilibrium, and which yields rather small transverse velocities [17].

In conclusion, we feel that photon interferometry can be used to obtain accurate information about the space-time dynamics of quarks and gluons in high energy nuclear collisions.

ACKNOWLEDGMENTS

The author would like to thank T. Awes, P. Braun-Munzinger, C. Gale, H. Gutbrod, A. H. Hirsch, L. McLerran, F. Plasil, N. T. Porile, R. P. Scharenberg, B. Sinha, and C. Y. Wong for stimulating conversations. He is grateful to J. I. Kapusta for a careful reading of the manuscript and for many useful suggestions. He is also grateful to M. Kataja and P. V. Ruuskanen for making their transverse expansion code available to him. This work was supported by the Minnesota Supercomputer Institute and U.S. Department of Energy under Grant No. DOE/DE-FG02-87ER40328.

- [1] K. Geiger, Phys. Rev. D **46**, 4965 (1992); **46**, 4986 (1992).
- [2] L. P. Csernai and J. I. Kapusta, Phys. Rev. Lett. **69**, 737 (1992).
- [3] D. Neuhauser, Phys. Lett. B **182**, 289 (1986).
- [4] Y. M. Sinyokov, in *Quark Matter '88*, Proceedings of the Seventh International Conference on Ultrarelativistic Nucleus-Nucleus Collisions, Lenox, Massachusetts, 1988, edited by G. Baym, P. Braun-Munzinger, and S. Nagamiya [Nucl. Phys. **A498**, 151c (1989)].
- [5] S. Raha and B. Sinha, Int. J. Mod. Phys. A **4**, 517 (1991).
- [6] D. K. Srivastava and J. I. Kapusta, Phys. Lett. B **307**, 1 (1993).
- [7] D. K. Srivastava and J. I. Kapusta, Phys. Rev. C **48**, 1335 (1993).
- [8] J. Kapusta, P. Lichard, and D. Seibert, Phys. Rev. D **44**, 2774 (1991); H. Nadeau, J. Kapusta, and P. Lichard, Phys. Rev. C **45**, 3034 (1992).
- [9] S. Chakrabarty, J. Alam, D. K. Srivastava, B. Sinha, and S. Raha, Phys. Rev. D **46**, 3802 (1992).
- [10] K. Kajantie, M. Kataja, L. McLerran, and P. V. Ruuskanen, Phys. Rev. D **34**, 2153 (1987).
- [11] J. Alam, D. K. Srivastava, B. Sinha, and D. N. Basu, Phys. Rev. D **48**, 1117 (1993).
- [12] H. von Gersdorff, M. Kataja, L. McLerran, and P. V. Ruuskanen, Phys. Rev. D **34**, 794 (1986).
- [13] J. D. Bjorken, Phys. Rev. D **27**, 140 (1983).
- [14] Y. M. Sinyokov, V. A. Averchenkov, and B. Lorstad, Z. Phys. C **49**, 417 (1991).
- [15] J. Kapusta, L. McLerran, and D. K. Srivastava, Phys. Lett. B **283**, 145 (1992).
- [16] D. K. Srivastava and B. Sinha, Phys. Lett. B **261**, 1 (1991); D. K. Srivastava, B. Sinha, M. Gyulassy, and X.-N. Wang, *ibid.* **276**, 285 (1992).
- [17] G. Bertsch, M. Gong, L. McLerran, P. V. Ruuskanen, and E. Sarkkinen, Phys. Rev. D **37**, 1202 (1989).